

Characterizing the coherence of Bose-Einstein condensates and atom lasers

R. J. Dodd†

*Institute for Physical Science and Technology,
University of Maryland at College Park, College Park, MD 20742.*

Charles W. Clark

*Electron and Optical Physics Division,
Physics Laboratory, National Institute of Standards and Technology, Technology
Administration, U. S. Department of Commerce, Gaithersburg, MD 20899-0001.*

Mark Edwards†

*Department of Physics, Georgia Southern University,
Statesboro, GA 30460-8031.*

K. Burnett†

*Clarendon Laboratory, Department of Physics, University of Oxford,
Parks Road, Oxford OX1 3PU, United Kingdom.*

bec@bruce.nist.gov

Abstract: For a dilute, interacting Bose gas of magnetically-trapped atoms at temperatures below the critical temperature T_0 for Bose-Einstein condensation, we determine the second-order coherence function $g^{(2)}(\mathbf{r}_1, \mathbf{r}_2)$ within the framework of a finite-temperature quantum field theory. We show that, because of the different spatial distributions of condensate and thermal atoms in the trap, $g^{(2)}(\mathbf{r}_1, \mathbf{r}_2)$ does not depend on $|\mathbf{r}_1 - \mathbf{r}_2|$ alone. This means that the experimental determinations of $g^{(2)}$ reported to date give only its spatial average. Such an average may underestimate the degree of coherence attainable in an atom laser by judicious engineering of the output coupler.

©1997 Optical Society of America

OCIS codes: (030.1640) Coherence; (140.3320) Laser cooling; (020.7010) Trapping

†Also at the Physics Laboratory, National Institute of Standards and Technology,
Technology Administration, U. S. Department of Commerce, Gaithersburg, MD 20899.

References and links

1. M. H. Anderson, J. R. Ensher, M. R. Matthews, C. E. Wieman, and E. A. Cornell, "Observation of Bose-Einstein condensation in a dilute atomic vapor," *Science* **269**, 198 (1995).
2. K. B. Davis, M.-O. Mewes, M. R. Andrews, N. J. van Druten, D. S. Durfee, D. M. Kurn, and W. Ketterle, "Bose-Einstein condensation in a gas of sodium atoms," *Phys. Rev. Lett.* **75**, 3969 (1995).
3. C. C. Bradley, C. A. Sackett, and R. G. Hulet, "Bose-Einstein condensation in lithium: observation of limited condensate number," *Phys. Rev. Lett.* **78**, 985 (1997).
4. M.-O. Mewes, M. R. Andrews, D. M. Kurn, D. S. Durfee, C. G. Townsend, and W. Ketterle, "An output coupler for Bose condensed atoms," *Phys. Rev. Lett.* **78**, 582 (1997).
5. M. R. Andrews, C. G. Townsend, H.-J. Miesner, D. S. Durfee, D. M. Kurn, and W. Ketterle, "Observation of interference between two Bose condensates," *Science* **275**, 637 (1997).
6. H. M. Wiseman, "Defining the (atom) laser," *Phys. Rev. A* (1997 in press).
7. E. A. Burt, R. W. Ghrist, C. J. Myatt, M. J. Holland, E. A. Cornell, and C. E. Wieman, "Coherence, correlation and collisions: what one learns from Bose-Einstein condensates from

- their decay,” *Phys. Rev. Lett.* **79**, 337 (1997).
8. W. Ketterle and H.-J. Miesner, “Coherence properties of Bose condensates and atom lasers,” *Phys. Rev. A* **57**, 3291 (1997).
 9. R. J. Dodd, K. Burnett, M. Edwards, and C. W. Clark, “Two-gas description of dilute Bose-Einstein condensates at finite temperature,” *Phys. Rev. A* (submitted).
 10. O. Penrose and L. Onsager, “Bose-Einstein condensation and liquid helium,” *Phys. Rev.* **104**, 576 (1956).
 11. D. F. Walls, “Evidence for the quantum nature of light,” *Nature* **280**, 451 (1979).
 12. R. Glauber, “Optical coherence and photon statistics,” in *Quantum Optics and Electronics*, C. DeWitt, A. Blandin, and C. Cohen-Tannoudji, eds. (Gordon and Breach, New York, 1965).
 13. A. L. Fetter, “Nonuniform states of an imperfect Bose gas,” *Ann. Phys.* (NY) **70**, 67 (1972).
 14. E. M. Lifshitz and L. P. Pitaevski, *Statistical Physics Part 2* (Butterworth Heinemann, Oxford, 1995).
 15. V. N. Popov, *Functional Integrals and Collective Modes* (Cambridge University Press, New York, 1987), Chapter 6.
 16. A. Griffin, “Conserving and gapless approximations for an inhomogeneous Bose gas at finite temperatures,” *Phys. Rev. B* **53**, 9341 (1996).
 17. M. Houbiers and H. T. C. Stoof, “Stability of Bose condensed atomic ${}^7\text{Li}$,” *Phys. Rev. A* **54**, 5055 (1996).
 18. Yu. Kagan, B. V. Svistunov, and G. V. Shlyapnikov, “Effect of Bose condensation on inelastic processes in gases,” *JETP Lett.* **42**, 210 (1985).
 19. H. T. C. Stoof, A. M. L. Janssen, J. M. V. A. Koelman, and B. J. Verhaar, “Decay of spin-polarized atomic hydrogen in the presence of a Bose condensate,” *Phys. Rev. A* **39**, 3157 (1989).
 20. R. Feynman, *Statistical Mechanics* (W. A. Benjamin, Reading, MA, 1972).
 21. S. R. de Groot, G. J. Hooyman, and C. A. ten Seldam, “On the Bose-Einstein condensation,” *Proc. R. Soc. London, Ser. A* **203**, 266 (1950).
 22. V. Bagnato, D. E. Pritchard, and D. Kleppner, “Bose-Einstein condensation in an external potential,” *Phys. Rev. A* **35**, 4354 (1987).
 23. D. A. W. Hutchinson, E. Zaremba, and A. Griffin, “Finite temperature excitations of a trapped Bose gas,” *Phys. Rev. Lett.* **78**, 1842 (1997).
 24. M. J. Holland and J. Cooper, “Expansion of a Bose-Einstein condensate in a harmonic potential,” *Phys. Rev. A* **53**, R1954 (1996).
 25. M. Edwards, R. J. Dodd, C. W. Clark, P. A. Ruprecht, and K. Burnett, “Properties of a Bose-Einstein condensate in an anisotropic harmonic potential,” *Phys. Rev. A* **53**, R1950 (1996).
 26. M. Edwards, P. A. Ruprecht, K. Burnett, R. J. Dodd, and C. W. Clark, “Collective excitations of Bose-Einstein condensates,” *Phys. Rev. Lett.* **77**, 1671 (1996).
 27. S. Stringari, “Collective excitations of a trapped Bose-condensed gas” *Phys. Rev. Lett.* **77**, 2360 (1996).
 28. Y. Castin and R. Dum, “Bose-Einstein condensates in time-dependent traps,” *Phys. Rev. Lett.* **77**, 5315 (1996).
 29. M. J. Holland, D. S. Jin, M. L. Chiofalo, and J. Cooper, “Emergence of interaction effects in Bose-Einstein condensation,” *Phys. Rev. Lett.* **78**, 3801 (1997).
 30. S. Giorgini, L. P. Pitaevskii, and S. Stringari, “Condensate fraction and critical temperature of a trapped interacting Bose gas,” *Phys. Rev. A* **54**, R4633 (1996).
 31. A. Minguzzi, S. Conti, and M. P. Tosi, “The internal energy and condensate fraction of a trapped interacting Bose gas,” *J. Phys.: Condens. Matter* **9**, L33 (1997).
 32. R. J. Dodd, M. Edwards, C. W. Clark, and K. Burnett, “Collective excitations of Bose-Einstein condensed gases at finite temperatures,” *Phys. Rev. A* (in press).

1. Introduction

The experimental demonstration of Bose-Einstein condensation (BEC) in magnetically-trapped atomic gases [1, 2, 3] has focused interest on the prospects for constructing a source of coherent matter waves, or “atom laser.” Indeed, a prototype device of this type has recently been demonstrated, [4] and the first-order coherence properties of BEC atom-sources have been demonstrated by the observation of interference fringes in collisions of separately prepared BECs. [5] There is some controversy over the use of the laser analogy to describe such systems, [6] in part because the theory of coherence has not yet been as fully developed for matter-wave as for optical-wave sources. Nevertheless, the rapid progress of this field has motivated practical definitions of matter-wave coherence based on optical analogies, and recent papers have presented determinations of coherence functions of BEC systems based on measurements of three-body decay rates [7] and measurements of the release energies of trapped gases.[8] We believe that a first-principles model of matter-wave coherence is needed to provide a framework within which the results of such experiments can be quantified. This paper presents an outline of such a theory, and describes several qualitative implications that the theory presents for future experiments.

Our treatment is based on a straightforward application of the quantum field theory of atoms, and it leads to one key result that appears to be of general validity. Current BEC systems are produced in atom traps, and so they are intrinsically inhomogeneous. Thus, measurements of coherence functions, such as those given in Burt *et al.* [7] and Ketterle and Miesner, [8] are actually determinations of the average of a local coherence function over an extended inhomogeneous system. Moreover, the condensed and non-condensed (“thermal”) fractions of the atomic gas are distributed differently over the trap, and they make separate and distinct contributions to the local coherence function. In simple models of a dilute interacting gas, we show that the local coherence function is related directly to the spatially-resolved condensate fraction $f(\mathbf{r})$ of the gas. For Bose gases with repulsive pair interactions (scattering length $a > 0$), the condensed and thermal components of the gas are largely segregated: the condensate is localized near the center of the trap, from which it expels the thermal cloud by the repulsive interaction. [9] Thus, even for systems that measurements show to have a significant net fraction of thermal atoms, it may be possible to selectively extract an atomic beam with the coherence properties of a nearly pure condensate by using an appropriately designed output coupling scheme.

We proceed by outlining the quantum field theory of the second-order coherence function, treating the equal-time or stationary case as this is of greatest interest to current experiments. The formalism is applied in explicit calculations of two cases: an ideal Bose gas in a spherical trap; and an interacting ^{87}Rb gas in the JILA TOP trap. [1] Similar results obtained for the third-order coherence function will be presented elsewhere.

2. Coherence of matter waves

When a Bose gas undergoes condensation there are changes in its first-order coherence function. In fact, the appearance of the condensate induces off-diagonal, long-range order (ODLRO), as explained by Penrose and Onsager. [10] In company with the optical case we come across the point of view [11] that a coherent laser field cannot be distinguished through its first-order coherence function from a filtered chaotic field of a thermal source: for example, one sees the same Young’s double-slit interference patterns from a laser as from a conventional light source. In the case of the gas we might then be led to observe that a condensate is, as far as its first-order, equal-time, matter-wave co-

herence function is concerned, equivalent to a filtered (but remarkably intense) chaotic deBroglie wave source.

The second-order coherence function arises in optics as a descriptor of the correlation between two separate photon-detection events, and, as emphasized by Walls [11], it is among the most elementary constructs that provides a clear contrast between quantum-mechanical and classical descriptions of the radiation field. So also in the case of atoms, the second-order coherence function shows unequivocal effects of Bose-Einstein condensation; thus it highlights the distinctions of the quantum-field-theoretical properties of a BEC *vs.* those of matter waves from a thermal source.

We now derive the zero-separation, equal-time, second-order coherence function for matter fields, presenting it in terms equivalent to those used by Glauber [12] to treat optical fields. We work within the framework of the Popov approximation to Hartree-Fock-Bogoliubov theory, [13, 14, 15, 16] as defined by Griffin. [16] As discussed in Sec. 4, this theory has been found to give an excellent description of the thermodynamics of the partially-condensed Bose gas, and, at least for condensate fractions above about 50%, a good account of condensate collective excitation frequencies. However, we note that the theory of the finite-temperature Bose gas still has many open questions.

The second-order coherence function is defined as [12]

$$g^{(2)}(\mathbf{r}_1, \mathbf{r}_2) = \frac{\langle \hat{\psi}^\dagger(\mathbf{r}_1) \hat{\psi}^\dagger(\mathbf{r}_2) \hat{\psi}(\mathbf{r}_2) \hat{\psi}(\mathbf{r}_1) \rangle}{\langle \hat{\psi}^\dagger(\mathbf{r}_1) \hat{\psi}(\mathbf{r}_1) \rangle \langle \hat{\psi}^\dagger(\mathbf{r}_2) \hat{\psi}(\mathbf{r}_2) \rangle}, \quad (1)$$

where $\hat{\psi}(\mathbf{r}_i)$ is the Bose field operator which annihilates an atom at position \mathbf{r}_i . The Bose field operators obey the usual commutation relations

$$[\hat{\psi}(\mathbf{r}_1), \hat{\psi}^\dagger(\mathbf{r}_2)] = \delta(\mathbf{r}_1 - \mathbf{r}_2), \quad [\hat{\psi}(\mathbf{r}_1), \hat{\psi}(\mathbf{r}_2)] = [\hat{\psi}^\dagger(\mathbf{r}_1), \hat{\psi}^\dagger(\mathbf{r}_2)] = 0. \quad (2)$$

Under the Popov approximation, the confined Bose gas is portrayed as a thermodynamic equilibrium system under a restricted grand canonical ensemble [17] whose thermodynamic variables are N , the total number of trapped atoms; T , the absolute temperature; and either N_0 , the number of condensate atoms, or μ , the chemical potential. The system Hamiltonian has the form

$$K \equiv H - \mu N = \int d\mathbf{r} \hat{\psi}^\dagger(\mathbf{r})(H_0 - \mu)\hat{\psi}(\mathbf{r}) + \frac{U_0}{2} \int d\mathbf{r} \hat{\psi}^\dagger(\mathbf{r})\hat{\psi}^\dagger(\mathbf{r})\hat{\psi}(\mathbf{r})\hat{\psi}(\mathbf{r}), \quad (3)$$

where $H_0 = -\frac{\hbar^2}{2M}\nabla^2 + V_{\text{trap}}(\mathbf{r})$ is the bare trap Hamiltonian, with trapping potential given by $V_{\text{trap}}(\mathbf{r}) = M(\omega_\rho^2 \rho^2 + \omega_z^2 z^2)/2$, with ω_ρ and $\omega_z = \sqrt{8}\omega_\rho$ being the radial and axial trap frequencies; and $U_0 = 4\pi\hbar^2 a/M$ is a measure of the interaction strength between atoms, with a being the scattering length for zero-energy binary atomic collisions.

The Bose field operator is written as the sum of a c -number condensate wave function, $\psi(\mathbf{r})$, and a fluctuation term, $\tilde{\psi}(\mathbf{r})$ which can be decomposed into a sum of quasi-particle modes

$$\hat{\psi}(\mathbf{r}) = \psi(\mathbf{r}) + \tilde{\psi}(\mathbf{r}) = \psi(\mathbf{r}) + \sum_j \left[u_j(\mathbf{r})\alpha_j + v_j^*(\mathbf{r})\alpha_j^\dagger \right]. \quad (4)$$

where α_j^\dagger and α_j are operators that, respectively, create and destroy the j^{th} mode. These operators satisfy the following commutation relations

$$[\alpha_j, \alpha_k^\dagger] = \delta_{jk}, \quad [\alpha_j, \alpha_k] = [\alpha_j^\dagger, \alpha_k^\dagger] = 0. \quad (5)$$

When the quasi-particle amplitudes, $u_j(\mathbf{r})$ and $v_j(\mathbf{r})$ satisfy Eqs. (13), the Popov Hamiltonian has the diagonal form

$$\hat{K} = \sum_j E_j \alpha_j^\dagger \alpha_j. \quad (6)$$

The ensemble average of an operator \hat{O} is given by [13]

$$\langle \hat{O} \rangle = \frac{\text{Tr} [\hat{O} e^{-\beta \hat{K}}]}{\text{Tr} [e^{-\beta \hat{K}}]}. \quad (7)$$

From this equation it is clear that $\langle \tilde{\psi} \rangle = 0$ and products of three $\tilde{\psi}$ operators will vanish as well as they consist of sums containing products either one or three quasi-particle creation and annihilation operators.

We decompose the field operator and expand the numerator in Eq. (1) evaluated at zero separation ($\mathbf{r}_1 = \mathbf{r}_2 \equiv \mathbf{r}$) and take the ensemble average. Under the Popov approximation anomalous averages such as $\langle \tilde{\psi} \tilde{\psi} \rangle$ are assumed negligible, after some algebra we find that

$$g^{(2)}(\mathbf{r}, \mathbf{r}) = 1 + \frac{1}{n(\mathbf{r})} \left\{ 2 |\psi(\mathbf{r})|^2 \tilde{n}(\mathbf{r}) + \tilde{n}^2(\mathbf{r}) \right\}. \quad (8)$$

In the above equation, $\tilde{n}(\mathbf{r}) = \langle \tilde{\psi}^\dagger(\mathbf{r}) \tilde{\psi}(\mathbf{r}) \rangle$ is the thermal-atom density and $n(\mathbf{r}) = |\psi(\mathbf{r})|^2 + \tilde{n}(\mathbf{r})$ is the total density. The coherence function can then be written in the simple form

$$g^{(2)}(\mathbf{r}, \mathbf{r}) = 2 - f^2(\mathbf{r}), \quad (9)$$

where $f(\mathbf{r}) = |\psi(\mathbf{r})|^2/n(\mathbf{r})$, the spatially resolved condensate fraction, is the ratio of the condensate density to the total density at position \mathbf{r} . This equation is relevant to recent experiments such as the determination of decay rates [7, 18, 19] and expansion energies. [8] It also agrees in the appropriate limit with that for a homogeneous gas, [19] where f , the condensate fraction, is independent of \mathbf{r} ; in that case, $g^{(2)}$ is simply a function of temperature T . However, as we have suggested above and shall show below, in current experiments $f(\mathbf{r})$ depends strongly upon \mathbf{r} . Note that $g^{(2)}(\mathbf{r}, \mathbf{r}) = 2$ for a thermal gas without condensation and $g^{(2)}(\mathbf{r}, \mathbf{r}) = 1$ for a pure BEC.

3. Second-order coherence of the ideal trapped Bose gas

We first outline the behavior of the second-order coherence function for an ideal Bose gas of atoms of mass M confined in a spherical harmonic potential with angular frequency ω ; the next section treats the effects of interactions and trap anisotropy. The spatially-resolved condensate fraction $f(\mathbf{r}) \equiv f(r)$ for the noninteracting trapped gas at temperature T can be computed directly from known results for the harmonic oscillator system: [20]

$$f(r) = \left[\frac{1}{N_0} \sum_{k=1}^{\infty} \frac{e^{-\beta k(\epsilon_0 - \mu)}}{[1 - e^{-2\beta k \hbar \omega}]^{3/2}} e^{(r/d)^2 \{1 - \tanh(\beta k \hbar \omega / 2)\}} \right]^{-1}, \quad (10)$$

where N_0 is the number of condensate atoms, $\epsilon_0 = \frac{3}{2} \hbar \omega$ is the ground-state energy of a single atom in the trap, $\beta = 1/k_B T$ with k_B being the Boltzmann constant, μ is the chemical potential, and $d = \sqrt{\hbar/M\omega}$ is the characteristic length scale of the single-atom ground state wavefunction, which in this case is the same as the condensate wavefunction

(in the discussion of anisotropic traps, our definition of d uses the geometric mean of the trap frequencies). In the low-temperature limit $\beta\hbar\omega \gg 1$, we find that $f(r)$ reduces to a form in which we can identify a characteristic length, $R(T)$, at which $f(R) = 1/2$:

$$R(T) = d e^{\beta\hbar\omega/2} \left(\frac{\ln[N_0]}{2} \right)^{1/2}, \quad (11)$$

where Figure 1 shows a false-color plot of $g^{(2)}(r) \equiv g^{(2)}(\mathbf{r}, \mathbf{r})$ vs. reduced temperature, T/T_0 , for $N = 40,000$ ^{87}Rb atoms in a spherical trap with $\nu = \omega/(2\pi) = 200$ Hz. Here T_0 is the critical temperature for an ideal trapped gas in the semiclassical limit; [21, 22] the transition temperatures of interacting, finite- N systems are somewhat lower than T_0 . The sharp blue \rightarrow red transition shows that $R(T)$ defines an appropriate length scale over a large range of temperatures, even though it was derived only in the low temperature limit, $T \ll \hbar\omega/k_B$, with $N_0 \gg 1$.

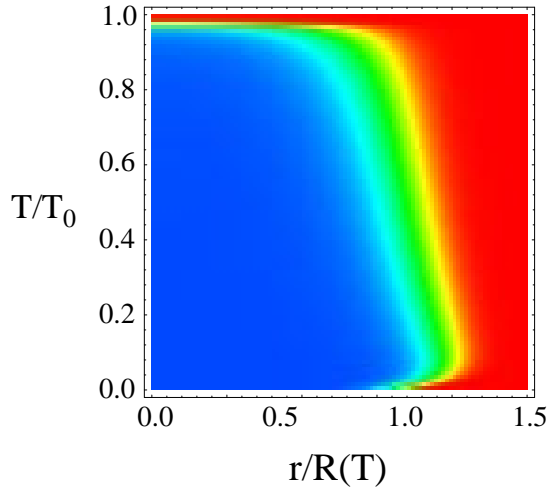


Figure 1. A false-color plot of $g^{(2)}(r)$ vs. reduced temperature, T/T_0 , and radial trap coordinate r , for $N = 40000$ ^{87}Rb atoms in a spherical trap with $\nu = 200$ Hz. The coherence length $R(T)$ is given by Eq. 11. Blue corresponds to $g^{(2)} = 1$ viz. coherence characteristic of a laser source; red to $g^{(2)} = 2$ viz. coherence characteristic of a thermal source. It is apparent that $R(T)$ defines the typical length scale over which laser-like coherence is maintained.

4. Interacting trapped gas

We have computed the second-order coherence function for a confined, interacting Bose gas using the Hartree-Fock-Bogoliubov (HFB) theory within an approximation originally introduced by Popov. [15, 16, 23] The HFB-Popov theory is a finite-temperature extension of Bogoliubov mean-field theory, which provides self-consistent treatment of the condensed and thermal components of the gas. The zero-temperature limit of this theory, which leads to the familiar Gross-Pitaevskii (GP) equation, has been found to describe accurately experimental values of condensate geometries, [24, 25] excitation frequencies, [26, 27, 28] and internal energies [29] for very cold condensates. The finite-temperature HFB-Popov treatment gives excellent agreement with experimental data on condensate fractions and transition temperatures [30, 31]; as for collective excitation frequencies, it appears to agree well with experiments for temperatures corresponding to thermal gas fractions of up to about 50%, though its validity at higher temperatures is uncertain. We have reported details of this approach and its comparison with

experiment in a separate publication, [32] and only summarize the underlying ideas here.

We treat systems of several thousand ^{87}Rb atoms in the JILA TOP trap. Following the approach of Sec. 2, we decompose the Bose field operator into a c -number condensate wave function plus an operator describing the non-condensate part: $\hat{\psi}(\mathbf{r}) = N_0^{1/2}\phi(\mathbf{r}) + \tilde{\psi}(\mathbf{r})$ and insert into Eq. (3). Linearization of this equation in the operators $\tilde{\psi}(\mathbf{r})$, leads [15, 16, 23, 32] to a generalized GP equation for $\phi(\mathbf{r})$

$$\left\{ H_0 + U_0 \left[N_0 |\phi(\mathbf{r})|^2 + 2\tilde{n}(\mathbf{r}) \right] \right\} \phi(\mathbf{r}) = \mu\phi(\mathbf{r}), \quad (12)$$

and to equations for quasi-particle amplitudes $u_j(\mathbf{r})$ and $v_j(\mathbf{r})$,

$$\begin{aligned} \mathcal{L}u_j(\mathbf{r}) + N_0U_0 |\phi(\mathbf{r})|^2 v_j(\mathbf{r}) &= E_j u_j(\mathbf{r}) \\ \mathcal{L}v_j(\mathbf{r}) + N_0U_0 |\phi(\mathbf{r})|^2 u_j(\mathbf{r}) &= -E_j v_j(\mathbf{r}), \end{aligned} \quad (13)$$

where where $\mathcal{L} \equiv H_0 + 2U_0 n(\mathbf{r}) - \mu$ and the E_j , the quasi-particle energies, are determined as eigenvalues. The quasi-particle amplitudes generate $\tilde{\psi}(\mathbf{r})$ via $\tilde{\psi}(\mathbf{r}) = \sum_j (u_j(\mathbf{r})\alpha_j + v_j^*(\mathbf{r})\alpha_j^\dagger)$, where $\alpha_j, \alpha_j^\dagger$ are quasi-particle annihilation and creation operators satisfying the usual Bose commutation relations.

The density of the thermal component of the gas $\tilde{n}(\mathbf{r})$ can be written in terms of the quasi-particle amplitudes as

$$\tilde{n}(\mathbf{r}) = \sum_j \left\{ \left[|u_j(\mathbf{r})|^2 + |v_j(\mathbf{r})|^2 \right] N_j + |v_j(\mathbf{r})|^2 \right\}, \quad (14)$$

where $N_j = (e^{\beta E_j} - 1)^{-1}$. The total number of trapped atoms, N , is given by

$$N = \int d\mathbf{r} n(\mathbf{r}) = N_0 + \int d\mathbf{r} \tilde{n}(\mathbf{r}). \quad (15)$$

Equations (12), (13), (14), and (15) form a closed system of equations that we refer to as the ‘‘HFB–Popov’’ equations (our version of Eq. (13) differs from that of Hutchinson *et al.* [23] via a sign change in the definition of $v_j(\mathbf{r})$). Numerical solution of these equations proceeds by choice of state variables $\{T, \mu, N\}$: for fixed T and μ , N is determined by solving the HFB–Popov equations, iteratively, to self-consistency.

Figure 2 shows the coherence function $g^{(2)}(\mathbf{r}, \mathbf{r})$ that emerges from such calculations for a sample of 2000 ^{87}Rb atoms in the JILA TOP trap with $\omega_\rho/(2\pi) = 74$ Hz at $T = 40$ nK, a temperature at which the condensate fraction is approximately 50%. The solid line shows the value of $g^{(2)}$ for the interacting sample, calculated by the HFB–Popov theory, and the dashed line shows the same calculation for a noninteracting sample. As can be seen, the repulsive atomic interactions extend the coherence length of the sample. This is due to two mechanisms: repulsive interactions between atoms of the condensate cause it to swell; and condensate atoms repel thermal atoms, leading to a more sharply defined variation of $f(\mathbf{r})$. These mechanisms are clearly manifested in the animated sequence of figures that follows below. Near the trap center, however, the ideal gas has a coherence closer to unity, since the peak density of a ideal gas condensate is substantially higher than that of an interacting one.

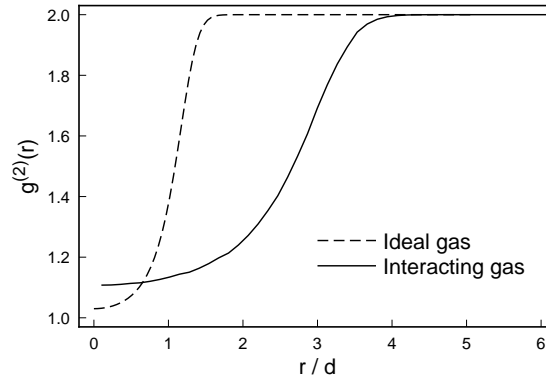


Figure 2. A plot of $g^{(2)}(r)$ versus r/d for 2000 ^{87}Rb atoms in the JILA TOP trap at 40 nK, with $\omega_\rho/(2\pi) = 74$ Hz. The figure displays the variation in the plane $z = 0$, with r being the cylindrical radius.

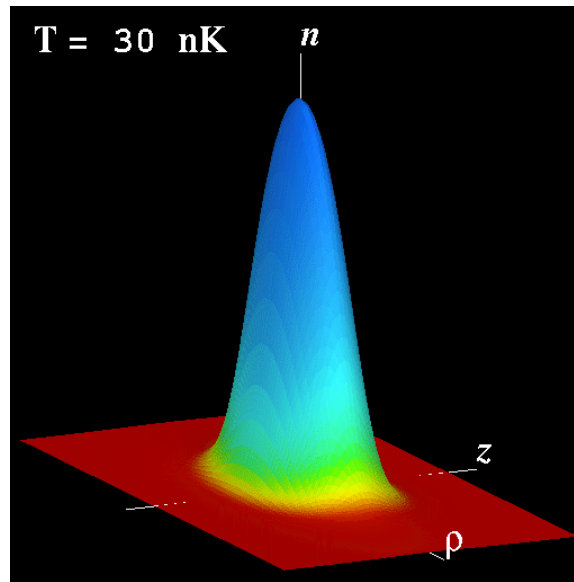


Figure 3. Animation of surface plots of the scaled total densities, $n(\mathbf{r})d^3$, versus ρ/d and z/d , for 2000 ^{87}Rb atoms in the JILA TOP trap with $\nu_\rho = 74$ Hz, at temperatures as labelled in each frame. The critical temperature T_0 for this system is ≈ 59 nK. The height of the surface is proportional to the density, the peak value displayed in these frames being $\approx 5 \times 10^{13}\text{cm}^{-3}$; the (dimensionless) z and ρ coordinates attain maximum values of 6 and 12, respectively; and the color shading represents the zero-separation, second-order coherence function of the system, $g^{(2)}(\mathbf{r}, \mathbf{r})$. Blue indicates high coherence ($g^{(2)} \sim 1$), while red indicates low coherence ($g^{(2)} \sim 2$).

Figure 3 shows an animated representation of the condensate density and spatially resolved second-order coherence function as a function of temperature for a condensate confined in the JILA TOP trap. The height of the plotted surface in each frame displays the *total* trapped-atom density in a plane that contains the trap axis, while the false-color shading exhibits the value of $g^{(2)}(\mathbf{r}, \mathbf{r})$. The blue-colored areas indicate laser-like coherence ($g^{(2)} = 1$), while red-colored areas depict thermal-like coherence ($g^{(2)} = 2$). Each frame of the animated sequence exhibits the density and coherence of the trapped atoms at a lower temperature than the previous one. The effect of the

thermal-atom density in this sequence of frames is quite subtle and can be discerned by watching the ρ and z axes as the animation progresses through the frames. One will see the ρ axis (white dotted line) being uncovered first (since the radial direction is more weakly confined than the axial direction in the JILA TOP trap) as T decreases followed by the uncovering of the z axis.

The above animation shows that the onset of a region containing coherent atoms is quite sudden and tends to occupy a large volume as T decreases. Furthermore, it is clear from this sequence that the condensate density (roughly the blue regions) far exceeds the thermal-atom density. The repulsion mechanisms discussed above are clearly in play.

5. Implications for experiment

We have shown that for a dilute Bose gas of magnetically-trapped atoms at temperatures below the critical temperature T_0 , the second-order coherence function $g^{(2)}(\mathbf{r}_1, \mathbf{r}_2)$ does not depend on $|\mathbf{r}_1 - \mathbf{r}_2|$ alone, as would be the case for a homogenous system. Instead, it exhibits significant dependence upon the trap spatial coordinates, and it reflects the relative purity of the condensate. For cases of repulsive interaction, regions of high relative purity are more extensive than those encountered in the ideal Bose gas.

Ketterle and Miesner [8] have noted that for a zero-range atomic pair interaction, the mean-field energy U of a Bose gas satisfies $U \propto \int d\mathbf{r} g^{(2)}(\mathbf{r}, \mathbf{r}) n^2(\mathbf{r})$. Experimental measurement of U can be made by observing the expansion of the gas upon dropping the trap. [29] If it is assumed that, as is the case in a homogeneous system, $g^{(2)}(\mathbf{r}, \mathbf{r})$ is independent of \mathbf{r} , *i.e.* $g^{(2)}(\mathbf{r}, \mathbf{r}) = g^{(2)}(0)$, then $g^{(2)}(0)$ can be obtained directly from experimental measurements of U and $n(\mathbf{r})$. A similar idea is employed by Burt *et al.*, [7] who infer a value of $g^{(3)}(0)$ from a three-body decay rate. However, according to the picture we have developed in this paper, the release-energy measurements actually determine a spatially-averaged value of $g^{(2)}(\mathbf{r}, \mathbf{r})$. Thus, the analysis of Ref. [8] gives $g^{(2)}(0) = [\int d\mathbf{r} g^{(2)}(\mathbf{r}, \mathbf{r}) n^2(\mathbf{r})] / [\int d\mathbf{r} n^2(\mathbf{r})]$, rather than a value of $g^{(2)}$ that characterizes the sample as a whole. For very cold samples that are nearly pure condensates, the density-weighted variance in the distribution of $g^{(2)}(\mathbf{r}, \mathbf{r})$ will be small, but quantitative investigations of the coherence properties of partially-condensed gases will have to account for effects of spatial dependence.

The expanded volume of high coherence that is induced by the condensate-cloud repulsion mechanism can have a positive impact on atom-laser design. For example, one scheme for out-coupling atoms from a condensate involves focussing two lasers into the condensate to cause transitions between trapped and untrapped magnetic sublevels via a two-photon Raman transition, and can in principle allow beam extraction from specific regions of the trap. Thus, even if one can only generate large condensates at relatively high temperatures, it may still be possible to extract a relatively pure condensate even in the presence of a substantial thermal component of the gas. In addition, we note that the effective segregation of condensate and non-condensate atoms may have favorable implications for loss rates associated with depolarizing atomic collisions. Two-body collisional rates are proportional to $g^{(2)}$, so there is a higher rate of collisional loss per unit density in the thermal cloud than in the condensate.

Acknowledgements

We thank John Hagedorn and Phillip Holman for their help in producing the figures. This work was supported in part by the U.S. National Science Foundation under grants PHY-9601261 and PHY-9612728, the U.S. Office of Naval Research, and the U. K. Engineering and Physical Sciences Research Council.